Optical transmission of periodic annular apertures in metal film on high-refractive index substrate: The role of the nanopillar shape

Optical transmission of periodic annular apertures in metal film on high-refractive index substrate: the role of a nanopillar shape

J.-S. Bouillard[1*] and J. Einsle[1], W. Dickson[1], S. G. Rodrigo[2], S. Carretero-Palacios[2], L. Martin-Moreno[2], F. J. Garcia-Vidal[3], A. V. Zayats[1]
[1] *Centre for Nanostructured Media, IRCEP, The Queen's University of Belfast, Belfast, BT7 1NN, United Kingdom*
[2] *Departamento de Física de la Materia Condensada, Facultad de Ciencias-ICMA, Universidad de Zaragoza-CSIC, E-50009 Zaragoza, Spain and*
[3] *Departamento de Física Teórica de la Materia Condensada, Universidad Autónoma de Madrid, Madrid 28049, Spain*

The influence of annular aperture parameters on the optical transmission through arrays of coaxial apertures in a metal film on high-refractive-index substrates has been investigated experimentally and numerically. It is shown that the transmission resonances are related to the plasmonic crystal effects rather than cut-off of annular apertures. The role of deviations from ideal aperture shape occurring during the fabrication process has also been studied. Annular aperture arrays are often considered in many applications for achieving high optical transmission through metal films and understanding of nanofabrication tolerances are important.

The so-called annular aperture arrays (AAA), consisting of subwavelength coaxial apertures in metal films, are currently considered as important extension of the plasmonic nanostructures for achieving the enhanced transmission of light through opaque materials.[1–6] Such nanostructures provide additional functionalities compared to simple circular apertures in terms of very high absolute transmission related to specific waveguided modes in annular apertures, absent in simple circular holes. Coupled to surface plasmon polariton modes on metal film interfaces, these modes provide a possibility to achieve high transmission, field enhancement as well as high extraction efficiency of light trapped in the substrates. The latter is especially important for high-refractive index substrates with small angles of total internal reflection. Therefore, such nanostructures may become important in a wide range of applications for light extraction from OLEDs, LEDs, VCSELs, etc.

At the same time, the studies of the enhanced optical transmission through the plasmonic structures on high-refractive index substrates are virtually absent, despise their potential interest in applications. There have been studies considering AAA with glass as a substrate, in the near-infrared, and the visible regime.[1–6] Recently, it was experimentally demonstrated an enhanced transmission around 90%.[9] When glass is used a substrate, it is possible to take advantage of the resonance associated with the cutoff of the TE_{11} mode of individual annular apertures. However, in the case of high refractive index (e.g., n$\approx$ 3.59 for GaAs or GaP), this resonance appears at much longer wavelengths, as it was reported from experiments in the THz regime.[10]

In this letter we present systematic studies of the enhanced transmission through the annular aperture arrays and its dependence on size, shape and period of the plasmonic nanostructures on high refractive index substrates that allows to emulate the plasmonic structures on LED chips. The influence of nanofabrication tolerances on optical properties of plasmonic AAA on high-index substrates are also studied.

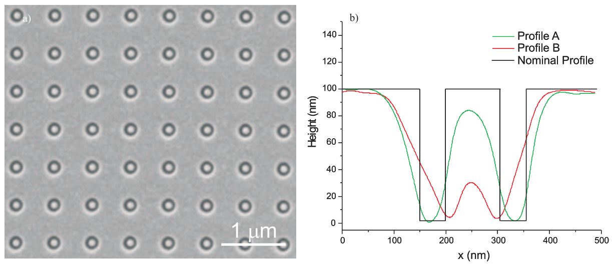

FIG. 1: (a) SEM image of a typical array of the FIB-milled annular apertures. (b) The cross-sections of AFM images showing the annular apertures profile for 100 nm inner diameter and 200 nm outer diameter apertures in the 600 nm period array milled with different FIB parameters.

We have studied annular aperture arrays fabricated in 100 nm thick Au film on the Gallium Phosphide (GaP) substrate (n = 3.14–3.59 in the visible spectral range). Four different type of the arrays of annular holes with a constant outer diameter of 200 nm and 4 different inner diameters: 0 nm (circular holes), 50 nm, 75 nm, and 100 nm. The square lattice arrays have been created with 3 different periods: 600 nm, 650 nm and 700 nm. The structures were fabricated using a Focussed Ion Beam (FIB) milling into magnetron sputtered Au films.

Scanning Electron Microscopy (SEM) and Atomic Force Microscopy (AFM) was used to characterise the structural integrity and parameters of the arrays. These confirmed good correspondence between the designed and actual parameters of the structures in terms of lateral sizes (Fig. 1 (a)). The profiles of the central pillar were, however, strongly dependent on the FIB milling parameters and for high beam currents, the FIB beam tail is too large to obtain a centre nanopillar with a height equal to that of the walls of the aperture. Therefore, in order to obtain the best shapes possible, low beam currents were used, typically 10 pA or 30 pA. The beam tail was also taken into account when creating the pattern file. However even considering these effects the ideal annular apertures are difficult to obtain on the required lengthscales (Fig. 1 (b)). Similar deviations and lack of control of the shape on such lengthscale are common also for other nanofabrication techniques such as nanoimprint and femtosecond 2-photon nanostructuring, that are most suitable for inexpensive mass-production of such arrays for photonic applications.

Optical characterisation was performed by measuring transmission spectra of the arrays at various angles of incidence and light polarisations. The light from a tungsten-halogen lamp was passed through a polarising cube before illuminating the sample, through the substrate. A pin hole was used to reduce the size of the illumination beam on the sample. A long-working-distance objective ($\times 50$) was used to collect the light transmitted through the structure. Part of the light passed through a beam splitter onto a CCD camera to visualise the illuminated area the sample surface, and the rest of the light was reflected onto an analysing polariser cube, with axis oriented parallel to the illumination polarisation, before being coupled into an optical fibre. The fibre was used to guide the optical signal to a spectrometer with a liquid nitrogen cooled CCD camera in order to record the spectrum of the transmitted optical signal.

For comparison to the experimental results, the zeroth order transmission spectra of each structure have been calculated using Finite-Difference Time-Domain method. The calculations were made taking into account a substrate with n = 3.59 covered with 100 nm of Au. The Au dielectric constant is taken form the experimental data (Ref.[11]) implemented in the FDTD formalism as described in Refs.[12,13]. The dispersion of the refractive index and absorption of GaP substrate were neglected for technical reasons, but the comparison with experiments shows that this is not an important effect.

The transmission spectra of the SPP crystals described above are presented in Fig. 2 for different parameters of the annular apertures and periods of the lattice. Please note that the strong extinction for wavelengths shorter than 550 nm is due to the strong absorption of GaP substrate in this spectral range.[14] The transmission spectra exhibit generally one dominating resonance with the period-dependent spectral position. The increase in the diameter of the inner pillar leads to the significant increase in the transmission magnitude despite the reduction of the total area of the openings. This is accompanied by a small long-wavelength shift of the transmission peak position. The maximum transmission was experimentally observed for annular aperture arrays with inner diameters of about 100 nm.

The spectra of the AAA milled with different parameters and therefore featuring different central nanopillar shape (Fig. 1 (b)) are shown in Fig. 2 (d). The nanopillars have different height and labelled "A" (tall) and "B" (small) as well as they have different effective diameter at approximately the same outer diameter of the annular

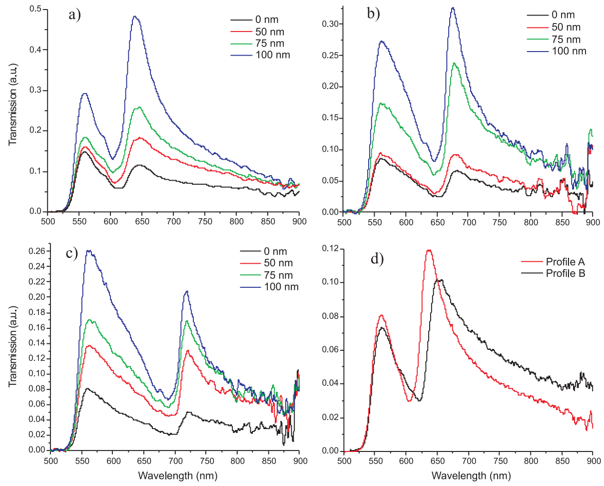

FIG. 2: Experimental transmission spectra of the aperture arrays fabricated in the 100 nm thick Au films on the GaP substrate for different periods of the array: (a) 600 nm, (b) 650 nm, (c) 700 nm. The outer diameter of the apertures are 200 nm, the inner diameters are indicated in the legends. (d) Experimental transmission spectra of the annular aperture arrays with different profiles of the central nanopillar, corresponding to the AFM images of Fig. 1(b).

aperture. While exhibiting similar spectrum defined by the SPP Bloch mode of the crystal, the resonant transmission of sample B is red-shifted and slightly smaller than for the array with taller nanopillars.

In the range of parameters of the plasmonic structures under consideration, the cut-off wavelength of individual annular holes are $\lambda_c = 590.5$ nm for the inner diameter equal to 50 nm and $\lambda_c = 1002$ nm for the inner diameter equal to 150 nm (Fig. 3). Therefore the observed resonances are not related to the cut-off of annular apertures. Simple analysis of plasmonic modes of our nanostructures shows that surface plasmon polaritons (SPPs) are not supported on the GaP/Au interface in the visible spectral range, since $\varepsilon_{Au} + \varepsilon_{GaP} > 0$ for $\lambda < 620$ nm. Although SPPs exist at lower frequencies, their wavelength is much shorter than that at the Au/air interface and propagation length is small in the visible spectral range due to the high-refractive index of the GaP. This considerably simplifies the discussion of the transmission mechanisms that may involve waveguided modes (photonic and/or plasmonic) in annular apertures and SPP Bloch modes on the air/Au interface of the plasmonic crystal.[7] The waveguided modes transmit the energy of the incident light with efficiency depending on the thickness of the film as well as the inner and outer diameters of the annular apertures since the propagation constant of the mode depends on them. These waveguided mode is then hybridised with SPP Bloch modes of the crystal lattice which are then coupled to photons. Therefore, the modification of the lattice period leads to the modification of the spectral position of the available SPP Bloch states and their overlap with the waveguided mode. This

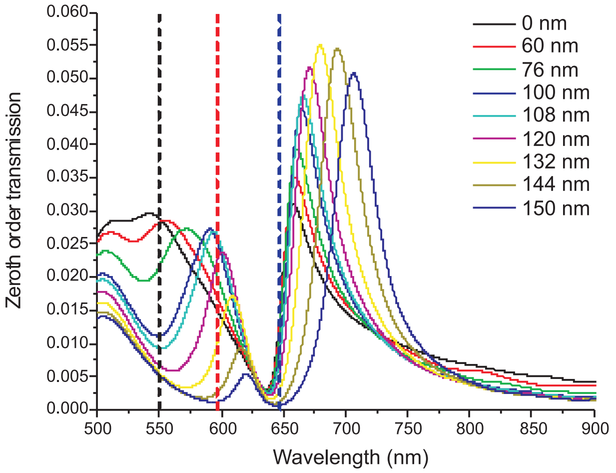

FIG. 3: Calculated transmission spectra of the annular aperture arrays in Au film for different diameters of the inner nanopillar. GaP substrate is considered dispersionless and lossless in the calculations. The film thickness is 100 nm, the period is 650 nm, the outer diameter of the apertures is 200 nm, the inner diameters are indicated in the legends. The dashed vertical lines indicate the cut-off wavelengths for holes and annular apertures of several inner diameters.

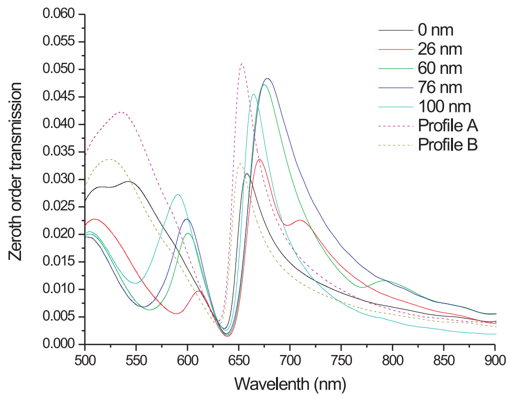

FIG. 4: Calculated transmission spectra of the annular aperture arrays in Au film for different heights of the inner nanopillar. GaP substrate is considered dispersionless and lossless in the calculations. The film thickness is 100 nm, the period is 650 nm, the outer diameter of the apertures is 200 nm, the inner diameter is 100 nm. The transmission spectra calculated for real nanopillar shapes as in Fig. 1(b) are also presented.

translates into both, red-shift of the transmission peak and the reduction of the absolute transmittance as the period increases.

Numerical modelling produce the transmission spectra and trends when the inner diameter and the pillar heights are varied, which are very similar to experimental observations (Figs. 3, 4). The spectra obtained with the ideal shapes of the apertures shows that the transmission increases in the dominating resonance with the increase of the nanopillar diameter. The position of the peak is strongly sensitive to the nanopillar diameter and exhibits strong red-shift when the nanopillar diameter becomes close to the aperture diameter. Since the absorption in the substrate is neglected, the second resonance is observed on the short-wavelength side of the SPP band-gap. A good agreement between theory and experiment is observed for the position of each transmission peak as well as the relative transmitted intensity for each structure. Please note that the experiment and modelling are compared for zeroth-order transmission; the calculated total transmission can be up to 20%.

The transmission spectra modelled for different heights of the central pillar are shown in Fig. 4. Again the increase of the nanopillar height leads to the increase of the transmission of the AAA. Initially, the resonance redshifts in comparison to the simple hole resonance until the nanopillar height is a half of the thickness of the film, for taller nanopillars the opposite trend with blueshift of the resonance is observed. The resonance on the short-wavelength side of the band-gap behaves however monotonically.

Finally, the modelling of the transmission spectra with real experimentally acquired profiles shows to recover almost perfectly the observed experimental spectra (Fig. 4). In these spectra the short wavelength peak near the absorption edge of the GaP is not resolved, and it is clear that the nanopillar profile and not the dispersion of the substrate is the reason. In both experiment and model, it is also clear that this peak is present as a broad shoulder. The interplay between the pillar height variation and the variations in the effective diameter, having opposite trends, minimise the shift of the resonant wavelength but have an impact on the absolute transmission.

In conclusion, we have studied the influence of the nanopillar shape on the resonant transmission through annular aperture arrays in Au film on high-refractive index substrate. Although a high-refractive index substrate prevent the efficient use of the SPP modes on Au/substrate interface for tailoring the transmission properties, the use of the nanostructure parameters allows to achieve some degree of tunability. At the same time, simplification of the available SPP Bloch mode spectrum leads to the observed spectral response which is robust to the fabrication tolerances while absolute transmission can be significantly influenced by them. Such AAA structures may find applications for light extraction and emission conditioning from semiconductor devices such as light-emitting diodes and VCSELs.

Acknowledgments

This work was supported in part by EPSRC (UK) and EC FP6 STREP PLEAS: Plasmon Enhanced Photonics. We would like to acknowledge the Spanish Ministry of Science under project MAT2008-06609-C02. The authors acknowledge fruitful discussions with R. Windisch.

---

* j.bouillard@qub.ac.uk

[1] F.I.Baida, D. Van Labeke, Phys. Rev. B 67, 155314 (2003).
[2] F.I. Baida, D. Van Labeke, G. Granet, A. Monoreau, App Phys B 79, 1 (2004).
[3] S.M. Orborn and A. Roberts, Opt. Express 14, 12623 (2006).
[4] F.I.Baida, A. Belkhir, D. Van Labeke, Phys Rev B 74, 205419 (2006).
[5] M. Haftel, C. Schlockermann, G. Blumberg, Phys Rev B 74 235405 (2006).
[6] J.Salvi, M.Roussey, F.I. Baida, M.-P. Bernal, A. Mussot, T. Sylvestre, H. Maillotte, D. Van Labeke, A. Perentes, I. Utke, C. Sandu, P. Hoffmann, and B. Dwir: Opt. Lett. 30, 1611 (2005).
[7] A.V. Zayats, I.I. Smolyaninov, and A.A. Maradudin, Phys. Rep. 408, 131 (2005).
[8] S.M. Orbons, D. Freeman, B. Lurther-Davies, B.C. Gibson, S.T. Huntington, D.N. Jamieson, A. Roberts, Physica B 394, 176 (2007).
[9] Y. Poujet, J. Salvi, F.I. Baida, Opt Lett 32, 2942 (2007).
[10] M. A. Seo, Opt. Express 16, 20484 (2008).
[11] P. B. Johnson and R. W. Christy, Phys. Rev. B 6, 4370 (1972).
[12] A. Vial, A. S. Grimault, D. Macias, D. Barchiesi, and M. L. de la Chapelle, Phys. Rev. B 71, 085416 (2005).
[13] S. G. Rodrigo, F. J. Garca-Vidal, and L. Martn-Moreno, Phys. Rev. B 77, 075401 (2008).
[14] E. D. Palik, Handbook of Optical Constants of Solids Academic, New. York (1985).